25th ABCM International Congress of Mechanical Engineering
October 20-25, 2019, Uberlândia, MG, Brazil

COBEM2019-2277
NONLINEAR TIME-STEP RESTRICTION ON MINIMAL GAIN MARCHING SCHEMES

Ricardo Dias dos Santos
Mariana Resende Volpini
Leonardo Santos de Brito Alves
Programa de Pós-Graduação em Engenharia Mecânica, Universidade Federal Fluminense, Rua Passo da Pátria 156, Bloco E, Sala 211, Niterói, RJ 24210-240, Brazil
ricardos@id.uff.br, marianavolpini@id.uff.br, leonardo.alves@mec.uff.br

Abstract. *When nonlinear stability properties must be preserved to maintain the shock-capturing capabilities of the chosen high-order spatial discretization, solution monotonicity is guaranteed by a time step restriction. Such a maximum nonlinear time step is more restrictive than its linear counterpart, even for time integration with implicit schemes, which can prevent the use of such schemes to generate steady-states with discontinuities, such as shock waves. Since minimal gain marching (MGM) schemes for steady-state generation are based on modifying the coefficients of marching schemes to minimize their linear gain at small time steps, the need to impose this nonlinear time step restriction can prevent the use of MGM schemes. Two classical test cases are used in this paper to evaluate how the coefficient modification required by MGM schemes to achieve linear gain minimization affects the maximum nonlinear time steps required for shock capturing, namely the shock formation modeled by the Burgers' equation and the Sod shock tube problem. In general, it was found that the nonlinear time step restriction is not significantly affected when using multi-step MGM schemes.*

Keywords: *Linear stability analysis, Total Variation Diminishing, Numerical analysis*

1. INTRODUCTION

Supersonic and hypersonic flight has been widely studied in the last decades. Many of these studies consist on the identification of mechanisms that trigger flow transition from a laminar to a turbulent state. This is relevant since key parameters, such as skin-friction and the heat-transfer rate, increase strongly during transition, having a big impact on the performance and structural safety of the vehicle itself.

Since shock waves are present in these flows, simulations with linearly stable finite difference schemes perform quite poorly, yielding numerical oscillations that deteriorate accuracy and can lead to divergence. In order to deal with this, new schemes have been developed to address nonlinear stability properties, such as total variation and entropy conditions (Harten, 1983), leading to Total Variation Diminishing (TVD) schemes (Boris and Book, 1973; van Leer, 1973).

These schemes with strong nonlinear stability should be combined with a time integration that preserves solution monotonicity, such as the forward Euler (FE) scheme. Hence, they were restricted to first-order accuracy in time. This difficulty led to the development of novel high-order time integration schemes (Shu and Osher, 1988). Originally called TVD time discretizations, they are known today as Strong Stability Preserving (SSP) schemes for time integration. They are also constructed as convex combinations of FE steps, which is responsible for the time step restriction $\Delta t \leq \mathcal{C}\,\Delta t_{FE}$ that guarantees their nonlinear stability properties. $\mathcal{C}$ is known as the SSP coefficient and a scheme is said to be SSP when $\mathcal{C} > 0$. Hence, a critical issue in the development of any given SSP scheme is the optimization process to determine the maximum allowable value of $\mathcal{C}$, which is what imposes a nonlinear time step restriction when using such schemes.

In the work of Ferracina and Spijker (2005) it is proven that implicit Runge-Kutta SSP schemes can be represented in the Butcher form. Under these circumstances, a Diagonally Implicit Runge-Kutta (DIRK) scheme may present an alternative to providing nonlinear stability while optimizing the linear gain.

The main idea behind the minimal gain marching schemes is that the coefficients of a marching scheme can be altered so it becomes linearly numerically stable under linearly physically unstable conditions. Achieving this at the smallest possible time steps prevents nonlinear effects from jeopardizing convergence towards steady-state. The first generation of MGM schemes was based on multi-step schemes (Teixeira and Alves, 2017). Two adjustable coefficients allow its linear gain to become smaller at smaller time steps when compared to the implicit Euler scheme. On the other hand, it should be mentioned that asymptotic, i.e. large time steps, linear gains do become larger.

None of the test cases studied so far with MGM schemes considered steady-states that posses discontinuities. For this reason, the work reported here analyzes the influence of linear gain minimization to generate steady-states on the nonlinear

time-step restriction imposed due to shock-capturing requirements. In other words, numerical tests are performed to verify if the maximum nonlinear time steps of MGM schemes are too small to allow the linear gain minimization required for steady-state generation. An in-house code is used to investigate these issues.

2. NUMERICAL METHODS

2.1 Strong Stability Preserving Methods

Strong Stability Preserving methods are high-order time discretization schemes that preserve nonlinear stability properties of first-order Euler time stepping. Gottlieb *et al.* (2011) concluded that this strong stability property guarantee is obtained whenever the time discretization can be decomposed into convex combinations of forward Euler steps. Therefore any convex functional property satisfied by forward Euler will be preserved by the higher-order time discretizations. Shu and Osher (1988) stated the concept of strong stability preserving methods, starting from a method of lines approximation of hyperbolic conservation laws such as equation

$$u_t = -f(u)_x \quad , \tag{1}$$

where the spatial derivative, $f(u)_x$, is discretized by a TVD finite difference and denoted by $-\mathcal{L}(u)$. In this manner, the spatial discretization has the property that when it is combined with the first-order forward Euler time discretization

$$u^{n+1} = u^n + \Delta t \mathcal{L}(u^n) \quad , \tag{2}$$

and for a sufficiently small time step, dictated by the Courant-Friedrichs-Levy (CFL) condition

$$\Delta t \leq \Delta t_{FE} \quad , \tag{3}$$

the total variation (TV) of the one-dimension discrete solution does not increase in time. In other words, the so-called TVD property holds:

$$TV(u^{n+1}) \leq TV(u^n) \quad , \tag{4}$$

$$TV(u^n) = \sum_j |u^n_{j+1} - u^n_j| \quad , \tag{5}$$

where

$$TV(u) = sup_{\Delta x} \int \left| \frac{u(x+\Delta x) - u(x)}{\Delta x} \right| \Delta x \quad , \tag{6}$$

with sup meaning supremum. Hence, the main goal of SSP methods is to maintain the strong stability property while achieving higher-order accuracy in time, perhaps with a modified CFL restriction (Shu *et al.*, 2001), such as

$$\Delta t \leq \mathcal{C} \Delta t_{FE} \quad . \tag{7}$$

2.2 Butcher Formularion

Runge-Kutta methods can be written as described by Butcher (2003)

$$u^{(i)} = u^n + \Delta t \sum_{j=1}^{s} a_{ij} \mathcal{L}^j \quad , \tag{8}$$

$$u^{n+1} = u^n + \Delta t \sum_{i=1}^{s} b_i \mathcal{L}^i \quad , \tag{9}$$

for $1 \leq i \leq s$, where $\mathcal{L}^i = \mathcal{L}(t_n + \Delta t\, c_i, u^{(i)})$. Alexander (1977) proved that formulations following

$$\begin{array}{c|c} \boldsymbol{c} & \boldsymbol{A} \\ \hline & \boldsymbol{b}^T \end{array} \quad \text{with} \quad \begin{array}{c|cc} \alpha & \alpha & \\ 1 & 1-\alpha & \alpha \\ \hline & 1-\alpha & \alpha \end{array} \quad \text{and} \quad \begin{array}{c|ccc} \alpha & \alpha & & \\ c_2 & c_2-\alpha & \alpha & \\ 1 & b_1 & b_2 & \alpha \\ \hline & b_1 & b_2 & \alpha \end{array} \quad , \tag{10}$$

are the only strongly S-stable ones of order two in two stages and order three in three stages, respectively, where $\alpha = 1 \pm \sqrt{2}/2$ for the former and $\alpha^3 - 3\alpha^2 + \frac{3}{2} - \frac{1}{6}$, lying in $(\frac{1}{6}, \frac{1}{2})$, $c_2 = (1+\alpha)/2$ and $b_1 = -(6\alpha^2 - 16\alpha + 1)/4$ for the latter. If one considers α as an arbitrary free parameter, where either b_1 or c_2 would be a free parameter as well, both schemes become first-order accurate but still remain Strongly S-Stable, which is desirable for steady-state calculations.

2.3 Multi-Step Minimal Gain Marching Scheme

The multi-step MGM scheme (Teixeira and Alves, 2017) control parameters should be set to $\theta_1 < 1$ and $\theta_2 > 2$ in order to enhance convergence towards steady-state. One should note that $\theta_1 = \theta_2 = 1$ leads to the implicit Euler scheme. Figure 1 shows the improved linear gain of this scheme, i.e.

$$\theta_1 \frac{q^{n+1} - q^n}{\Delta t} + (1 - \theta_1) \frac{q^{n+1} - q^{n-1}}{2\,\Delta t} = \theta_2\, \mathcal{L}^{n+1} + (1 - \theta_2)\, \mathcal{L}^n \quad , \tag{11}$$

when $\theta_1 = 1$ and $\theta_2 > 1$, noting that the linearization $\mathcal{L}^n = \lambda\, u^n$ was employed.

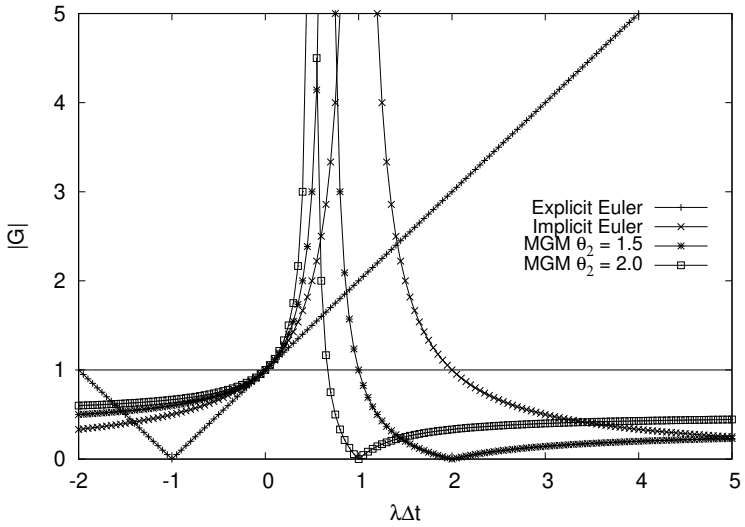

Figure 1. Gain comparison between traditional explicit and implicit with MGM schemes for $\theta_1 = 1$.

A key point analyzed in this work is the verification of the maximum nonlinear time step, as a function of θ_1 and θ_2, required to maintain the accurate shock-capturing capabilities of the spatial discretization. In doing so, it is hoped that both the linear steady-state generation mechanism used by MGM schemes, as well as nonlinear shock capturing capabilities, can be optimized simultaneously.

3. RESULTS

3.1 Linear case

From Eq. (10), the first-order accuracy requirement in the coefficient calculation allows one free parameter, α, for linear gain minimization both schemes. Considering a linear problem, one can write the gain as $G = u^{n+1}/u^n = e^{\lambda \Delta t}$, where the scheme is numerically stable whenever $|G| \leq 1$. Figures 2 and 3 show the linear gain for the implicit Euler

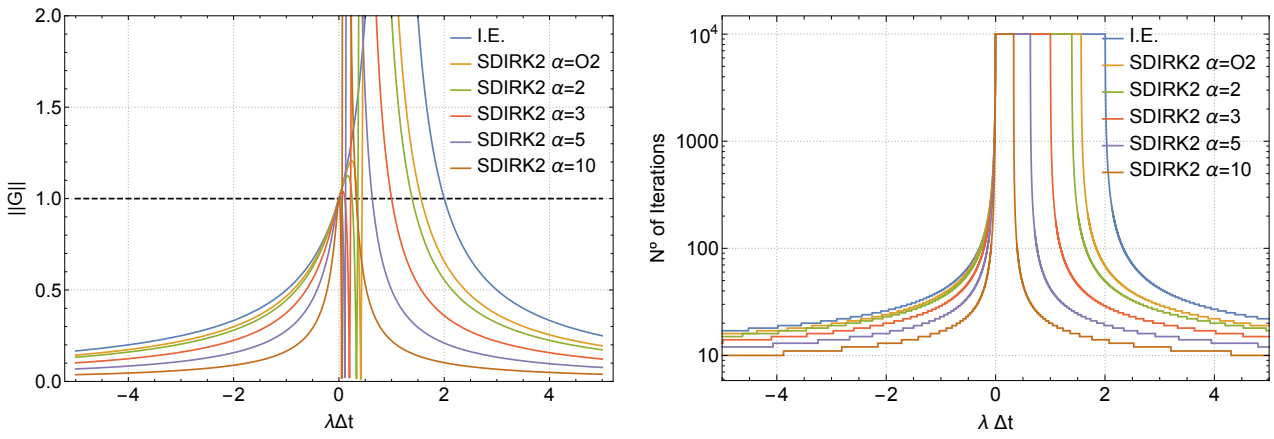

Figure 2. Absolute value of the gain (left) and total number of iterations for convergence (right) as functions of the dimensionless time step. Dashed lines indicate an approximate threshold for instability.

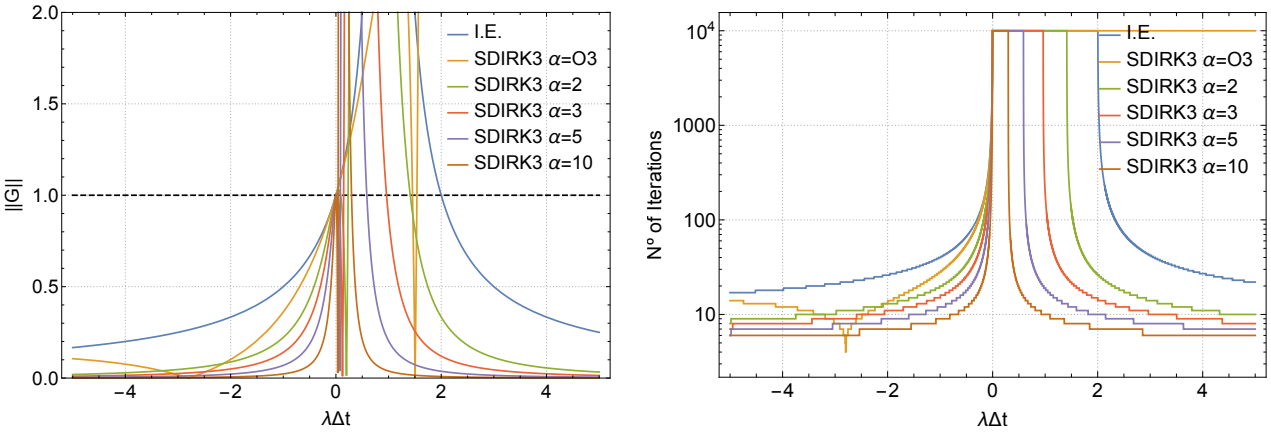

Figure 3. Absolute value of the gain (left) and total number of iterations for convergence (right) as functions of the dimensionless time step. Dashed lines indicate an approximate threshold for instability.

scheme as well as the DIRK schemes with two stages/second-order and three stages/third-order for different values of the free parameter. They indicate that the number of iterations required by each scheme to reach a steady-state with a tolerance of 10^{-12} for a linear problem follows the trends dictated by the linear gain of the respective scheme.

3.2 Scalar Conservation Law

The first nonlinear test case is based on the dimensionless inviscid Burgers' equation, obtained using $f(u) = u^2/2$ in Eq. (1). Figure 4 shows the time evolution considering $u^0(x) = \sin(2\pi x)$ as initial condition as well as $u(0,t) = u(1,t) = 0$ as boundary conditions. All simulations used a second-order TVD scheme for spatial discretization.

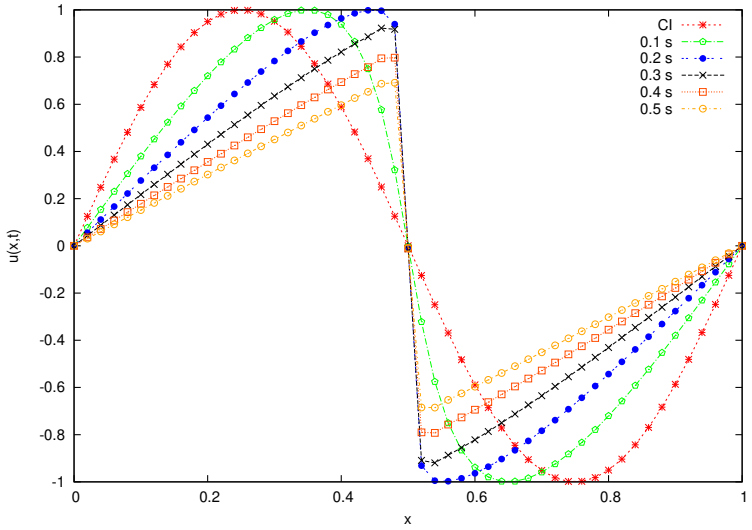

Figure 4. Velocity profile with $N_x = 51$ and $\Delta t = 10^{-3}$.

It is unknown how the nonlinear properties of these schemes respond when the Runge-Kutta coefficients are changed in order to minimize the linear gain. Since an entropic solution has a non-increasing total variation, i.e. $TV(u(\cdot,t)) \leq TV(u^0)$, the maximum nonlinear time-step allowed is measured by this condition. Figure 5 shows that the free parameter α has a big impact on this nonlinear time-step restriction. When increasing this parameter from one to seven in the three-stage scheme to minimize the linear gain, a three order of magnitude decay in the maximum nonlinear time step is observed. Furthermore, considering the three-stage scheme with two degrees of freedom, i.e. α and b_1, does not prevent this problem from occurring.

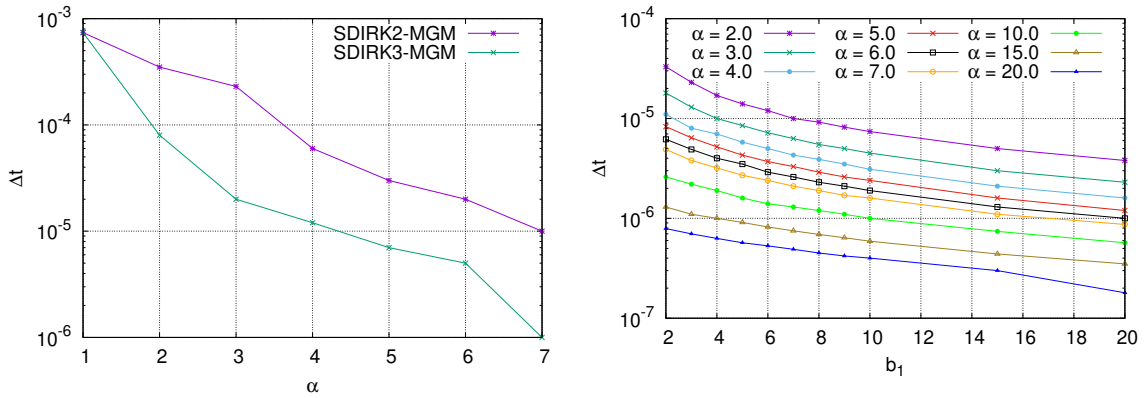

Figure 5. Maximum time-step possible that satisfy the Total variation condition. Scheme with one degree of freedom (left) and with two degrees of freedom (right).

For the multi-step minimal gain marching scheme, the maximum nonlinear time step does not vary significantly as the free parameters θ_1 and θ_2 are varied, as presented in Fig. 6. It is important to note that a quantitative criterion is used to calculate this nonlinear restriction. The maximum time step allowed by these schemes is chosen to prevent the total variation ratio between the solutions at the final and initial times simulated from becoming larger than one, so these solutions can still be considered entropic as indicated by Eq. 5 and shown in Fig. 7.

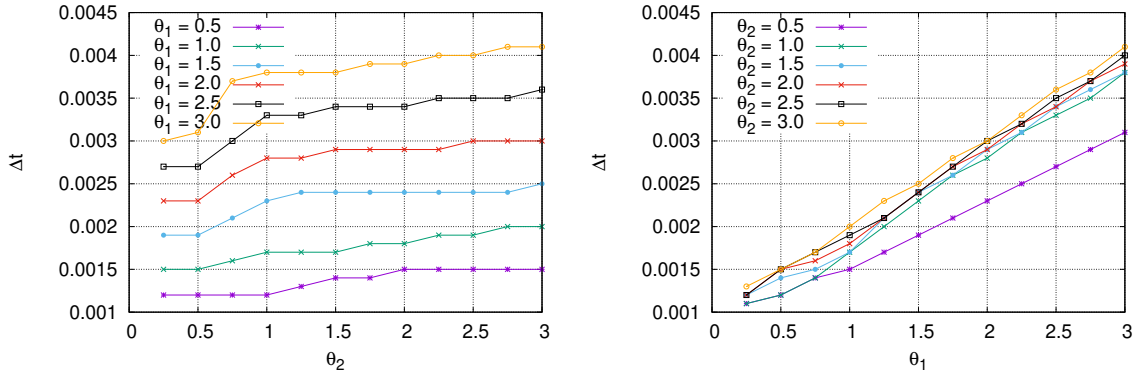

Figure 6. Maximum time step using GCN with $\theta_1 = 1.0$and $\theta_2 = 1.0$.

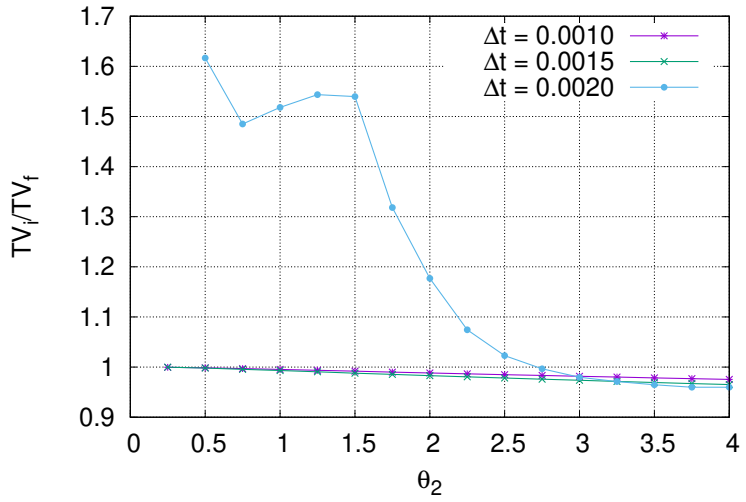

Figure 7. Total Variation ratio with $\theta_1 = 1.0$ and $N_x = 501$ points.

3.3 Compressible Euler

The second nonlinear test case considers the one dimensional Euler equation

$$\frac{\partial \mathbf{Q}}{\partial t} + \frac{\partial \mathbf{E}_i}{\partial x} = 0 \quad , \tag{12}$$

where $\mathbf{Q}$, the vector of conserved variables and $\mathbf{E}_i$, the flux vector are defined by,

$$\mathbf{Q} = \begin{bmatrix} \rho \\ \rho u \\ \rho e \end{bmatrix} \quad \text{and} \quad \mathbf{E}_i = \begin{bmatrix} \rho u \\ p + \rho u^2 \\ (\rho e + p)u \end{bmatrix} \quad , \tag{13}$$

with ρ, u, p and e being density, velocity, pressure and specific total energy respectively. These simulations consider the ideal gas law for air, $p = \rho RT$, with the specific gas constant $R = 287.053\ Jkg^{-1}K^{-1}$ and, alongside a ratio of specific heats $\gamma = 1.4$, the speed of sound $a = \sqrt{\gamma RT}$ can also be calculated. Furthermore, the Sod shock tube problem is analyzed. It considers a domain size of [-10, 10], N_x number of grid points in the domain and initial condition $\{p_L, \rho_L, u_L\} = \{10^5, 1.0, 0.0\}$ and $\{p_R, \rho_R, u_R\} = \{10^4, 0.125, 0.0\}$, all in S.I. units.

Considering the above properties, Fig. 8 (left) shows the density profile at $t = 10^{-2}$ obtained with the two-stage/second-order SDIRK method. On the other hand, Fig. 8 (right) presents the maximum nonlinear time step allowed by constraining the total variation, where all simulations used a second-order TVD scheme for spatial discretization, of the three-stage MGM scheme. It is clear that the maximum nonlinear time step decreases by a few orders of magnitude whenever the free parameters are varied to minimize the linear gain, when compared to the implicit Euler scheme. Such a behavior makes these schemes unsuitable to extract unstable and discontinuous steady-states from the compressible Euler equations.

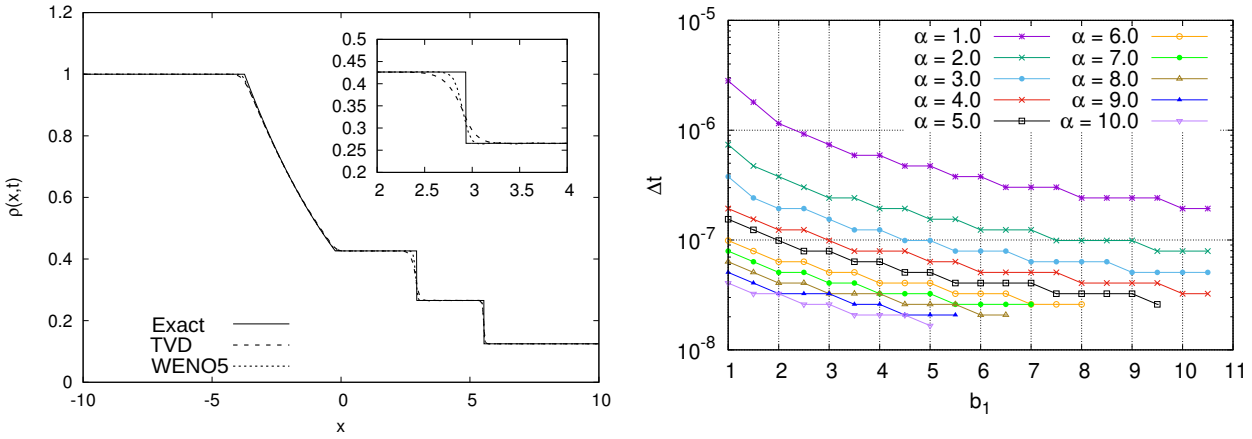

Figure 8. Density solution of Sod's problem with $N_x = 501$ at $t = 10^{-2}$ (left) and maximum time step for MGM-SDIRK3 scheme (right).

4. CONCLUSIONS

Steady-states are important in computational fluid dynamics, especially as initial conditions and reference solutions for sponge zones used in direct numerical simulations. They are also relevant for a wide range of stability analysis techniques. Traditional time marching schemes might not reach steady-states due to nonlinearities that prevent the time step from being chosen large enough values to place the physically unstable linear modes inside the numerically stable linear region of these schemes. MGM schemes were developed to overcome this difficulty, but the presence of discontinuities in these steady-states can prevent MGM schemes from generating them while maintaining their shock-capturing capabilities.

The multi-step MGM scheme was shown capable of simulating flows with discontinuities while being total variation diminishing for several values of the free parameters used to minimize the linear gain and enable steady-state generation. For the multi-stage MGM scheme tested here, on the other hand, the nonlinear time step restriction that maintains total variation prevents the time step from reaching high enough values to minimize the linear gain whenever the MGM free parameters are varied, making them unsuitable for the generation of steady-states with discontinuities.

5. ACKNOWLEDGEMENTS

MRV and LSBA gratefully acknowledge support of CNPq by project MCTI/CNPq - 307206/2016-5. RDS and LSBA would like to thank the support received from AFOSR (SOARD) Grant FA9550-18-1-0419. Any opinions, findings, and

conclusions or recommendations expressed in this material are those of the authors and do not necessarily reflect the views of the United States Air Force Office of Scientific Research or the United States Government.

6. REFERENCES

Alexander, R., 1977. "Diagonally implicit Runge-Kutta methods for stiff O.D.E."'. *SIAM Journal on Numerical Analysis*, Vol. 14, No. 6, pp. 1006–1021.

Boris, J.P. and Book, D.L., 1973. "Flux-corrected transport. i. SHASTA, a fluid transport algorithm that works". *Journal of Computational Physics*, Vol. 11, pp. 38–69.

Butcher, J.C., 2003. *Numerical Methods for Ordinary Differential Equation*. Wiley, England.

Ferracina, L. and Spijker, M.N., 2005. "Computing optimal monotonicity-preserving runge-kutta methods". Technical Report MI2005-07, Leiden University.

Gottlieb, S., Ketcheson, D. and Shu, C.W., 2011. *Strong Stability Preserving Runge-Kutta and Multistep Time Discretizations*. Word Scientific.

Harten, A., 1983. "High resolution schemes for hyperbolic conservation laws". *Journal of Computation Physics*, Vol. 49, pp. 357–393.

Shu, C.W., Gottlieb, S. and Tadmor, E., 2001. "Strong stability-preserving high-order time discretization methods". *SIAM Review*, Vol. 42, pp. 89–112.

Shu, C.W. and Osher, S., 1988. "Efficient implementation of essencially non-oscillatory shock capturing schemes". *Journal of Computational Physics*, Vol. 77, No. 2, pp. 439–471.

Teixeira, R.S. and Alves, L.S.B., 2017. "Minimal gain marching schemes: searching for unstable steady-states with unsteady solvers". *Theoretical and Computational Fluid Dynamics*, Vol. 31, No. 5, pp. 607–621.

van Leer, B., 1973. "Towards the ultimate conservative difference scheme i. the quest of monotonicity". In *Proceedings of the Third International Conference on Numerical Methods in Fluid Mechanics*. Vol. Fundamental Numerical Techniques of *Lecture Notes in Physics*, pp. 163–168.

7. RESPONSIBILITY NOTICE

The authors are the only responsible for the printed material included in this paper.